

Dissipation of energy in steel frames with PR connections

Alfredo Reyes-Salazar[†]

Facultad de Ingeniería, Universidad Autónoma de Sinaloa, Culiacan, Sinaloa, México

Achintya Haldar[†]

*Department of Civil Engineering and Engineering Mechanics,
University of Arizona, Tucson, AZ 85721, U.S.A.*

Abstract. The major sources of energy dissipation in steel frames with partially restrained (PR) connections are evaluated. Available experimental results are used to verify the mathematical model used in this study. The verified model is then used to quantify the energy dissipation in PR connections due to hysteretic behavior, due to viscous damping and at plastic hinges if they are formed. Observations are made for two load conditions: a sinusoidal load applied at the top of the frame, and a sinusoidal ground acceleration applied at the base of the frame representing a seismic loading condition. This analytical study confirms the general behavior, observed during experimental investigations, that PR connections reduce the overall stiffness of frames, but add a major source of energy dissipation. As the connections become stiffer, the contribution of PR connections in dissipating energy becomes less significant. A connection with a T ratio (representing its stiffness) of at least 0.9 should not be considered as fully restrained as is commonly assumed, since the energy dissipation characteristics are different. The flexibility of PR connections alters the fundamental frequency of the frame. Depending on the situation, it may bring the frame closer to or further from the resonance condition. If the frame approaches the resonance condition, the effect of damping is expected to be very important. However, if the frame moves away from the resonance condition, the energy dissipation at the PR connections is expected to be significant with an increase in the deformation of the frame, particularly for low damping values. For low damping values, the dissipation of energy at plastic hinges is comparable to that due to viscous damping, and increases as the frame approaches failure. For the range of parameters considered in this study, the energy dissipations at the PR connections and at the plastic hinges are of the same order of magnitude. The study quantitatively confirms the general observations made in experimental investigations for steel frames with PR connections; however, proper consideration of the stiffness of PR connections and other dynamic properties is essential in predicting the dynamic behavior.

Key words: energy dissipation; partially restrained connections; sinusoidal loading; viscous damping; hysteretic damping; inelastic analysis; MDOF elasto-plastic system; time history analysis; moment resisting steel frames; connection stiffness.

1. Introduction

The profession has known for a long time that the connections in a typical steel frame are essentially partially restrained (PR) with different rigidities. Thus, the dynamic behavior of steel frames with PR connections has been an important research topic. In the early nineties, several

[†] Professor

experimental works were undertaken to study the dynamic behavior of steel frames. Leon and Shin (1995) used sinusoidal loadings in their experimental investigations to study the changes in the behavior of steel frames due to the presence of PR connections as opposed to fully restrained (FR) connections. Nader and Astenah (1991) observed that the presence of PR connections reduced the lateral stiffness, but increased the energy dissipation at the PR connections. The amount of extra energy dissipation was not quantified. Since the energy dissipation characteristics of steel frames will dictate their dynamic behavior, it is highly desirable to quantify the contributions of different sources of energy dissipation and assess their relative significance. The intent of this paper is to provide a quantitative interpretation of information that is usually discussed qualitatively. The subject is addressed comprehensively in this paper.

2. Dissipation of energy

The energy imparted to a structure by any dynamic load is absorbed and dissipated by the structure through different mechanisms. The absorption mechanisms consist of the kinetic energy, including the rigid body translation of the structure and the elastic strain energy. The dissipation mechanisms traditionally considered in dynamic analysis of structures consist of the hysteretic behavior of the material at positions of plastic hinges and other nonyielding mechanisms, usually represented by equivalent viscous damping (Uang and Bertero 1990). For mathematical modeling, plastic hinges are considered to occur at locations where the combined action of the axial force and bending moments satisfy a prescribed yield function along the length of a member. This is discussed in detail elsewhere by Gao and Haldar (1995). Once a plastic hinge is formed, the energy dissipation process begins at that location. On the other hand, energy dissipation by viscous damping takes place during the whole period of excitation and is present even for small structural deformation.

It has been generally accepted that a structure can survive a dynamic load if the structural energy absorption and dissipation capacities are greater than the input energy (Kawamura and Galambos 1989). As stated earlier, the presence of PR connections in a steel structure will reduce its stiffness, but at the same time will increase the energy dissipation capacity, altering both the stiffness and damping characteristics of the structure. Thus, it is very important to explicitly address the energy dissipation at the PR connections, considering loading and unloading processes and variation with time. This is expected to produce a generally-overlooked form of hysteretic damping, which could be a very important source of energy dissipation in the structure, resulting in significant changes in the structural response.

Even though many studies have been carried out in the area of static analysis of frames with PR connections (Fry and Morris 1975, Chen and Liu 1987, Richard 1986) and a few studies have been conducted for the dynamic case (Haldar and Reyes-Salazar 1996, Colson 1991, El-Salti 1992), there has not been an explicit evaluation of the energy dissipation at PR connections. The main objective of this paper is to investigate the amount of energy that PR connections of steel frames can dissipate during dynamic loading, and its significance in comparison to the other sources of energy dissipation discussed earlier. To achieve this objective, a mathematical model is developed which can predict the results of laboratory experiments. Conceptually, any form of dynamic loading, including seismic loading, can be used for verification purposes. However, the use of very irregular seismic time histories to extract information for quantitative comparison is expected to be very

challenging. Thus, the sinusoidal experimental results reported by Leon and Shin (1995) are used in this study to calibrate the proposed model. The calibration of the model using seismic loading is now under consideration and will be reported in the near future. The verified model is used to quantify different sources of energy dissipation for both seismic and dynamic loadings. An extensive parametric study is then conducted to make some important observations.

3. Proposed Model

As stated earlier, the input energy (E_I) for a structure during dynamic loading at time interval t_1 and t_2 is absorbed by the elastic strain energy (E_S) and kinetic energy (E_K), and dissipated by viscous damping (E_D), hysteretic behavior of the material at plastic hinges (plastic energy, E_P), and the hysteretic behavior at PR connections (E_C) if they are considered in the mathematical model. This energy balance equation for the system can be mathematically represented as:

$$E_I = \Delta E_S + \Delta E_K + E_D + E_P + E_C \quad (1)$$

Each of the energy terms in Eq. (1) can in turn be expressed as discussed below.

The input energy for a given load $p(t)$ acting on the structure can be calculated as:

$$E_I = \int_{u_1}^{u_2} p(t) du = \int_{t_1}^{t_2} p(t) \dot{u} dt \quad (2)$$

where u is the displacement corresponding to $p(t)$.

The variation in the elastic strain energy is given by the following equation:

$$\Delta E_S = \left(\frac{1}{2} \mathbf{U}^T \mathbf{K}^t \mathbf{U} \right)_{t_2} - \left(\frac{1}{2} \mathbf{U}^T \mathbf{K}^t \mathbf{U} \right)_{t_1} \quad (3)$$

where \mathbf{K}^t is the tangent stiffness matrix of the structure and \mathbf{U} is the displacement vector.

The variation in the kinetic energy is obtained as:

$$\Delta E_K = \left(\frac{1}{2} \dot{\mathbf{U}}^T \mathbf{m} \dot{\mathbf{U}} \right)_{t_2} - \left(\frac{1}{2} \dot{\mathbf{U}}^T \mathbf{m} \dot{\mathbf{U}} \right)_{t_1} \quad (4)$$

where \mathbf{m} is the mass matrix and bold $\dot{\mathbf{U}}$ is the velocity vector.

The plastic energy at plastic hinges can be estimated by calculating the work done by the resultant stresses through the corresponding plastic deformations. For plane frames it can be expressed as (Haldar and Nee 1989):

$$E_P = \sum_{i=1}^n M_p \Theta_p + \sum_{i=1}^n P_p H_p \quad (5)$$

where n is the number of plastic hinges formed, \mathbf{M}_p and \mathbf{P}_p are the moment and axial force, respectively, acting on a plastic hinge, and Θ_p and H_p are the corresponding plastic rotation and plastic axial deformation, respectively. The summation is taken to consider the contributions of all

plastic hinges developed in the structure.

The energy dissipated by viscous damping is given by:

$$E_D = \int_{\dot{u}_1}^{\dot{u}_2} \mathbf{C} \dot{\mathbf{U}} \, du = \int_{t_1}^{t_2} \dot{\mathbf{U}}^T \mathbf{C} \dot{\mathbf{U}} \, dt \quad (6)$$

where \mathbf{C} is the viscous damping matrix of the structure.

Finally, the dissipation of energy at PR connections is estimated by considering the hysteretic behavior of moment, shear and axial forces. The energy dissipation due to moment at the PR connections, E_m , is calculated as:

$$E_m = \sum_{j=1}^m \left(\int_{\theta_1}^{\theta_2} M \, d\theta \right) = \sum_{j=1}^m \left(\int_{t_1}^{t_2} M \dot{\theta} \, dt \right) \quad (7)$$

where m is the number of PR connections in the structure, M is the connection moment and θ is the relative rotation of the connection. The summation is taken to consider the contributions of all the PR connections in the structure.

The energy dissipation due to shear force at the PR connections, E_v , is calculated as:

$$E_v = \sum_{j=1}^m \int_{\lambda_1}^{\lambda_2} V \, d\lambda = \sum_{j=1}^m \int_{t_1}^{t_2} V \dot{\lambda} \, dt \quad (8)$$

where V is the shear force and λ is the shear deformation.

The energy dissipation due to axial force at the PR connections, E_n , is calculated as:

$$E_n = \sum_{j=1}^m \int_{\delta_1}^{\delta_2} N \, d\delta = \sum_{j=1}^m \int_{t_1}^{t_2} N \dot{\delta} \, dt \quad (9)$$

where N is the axial force and δ is the axial deformation.

The total energy dissipation at the PR connections, E_c , can be estimated by adding Eqs. (7)-(9), i.e.:

$$E_c = E_m + E_v + E_n \quad (10)$$

4. Modeling of PR connection - The Richard Model

It is generally accepted that the comprehensive properties of a PR connection can be represented by its moment-relative rotation ($M - \theta$) curve. The Richard Model (1993) is adopted in this study to represent the behavior of the connections. This model is used because of its applicability to a wide variety of connections. This model is expressed as:

$$M = \frac{(K - K_p) \theta}{\left(1 + \left| \frac{(K - K_p) \theta}{M_0} \right|^N \right)^{\frac{1}{N}}} + K_p \theta \quad (11)$$

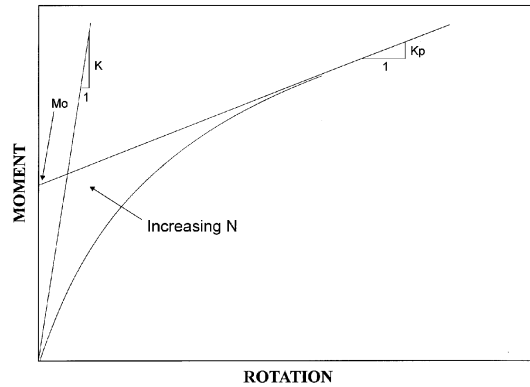


Fig. 1 Physical definition of Richard's Parameters

where M is the connection moment, θ is the connection rotation, K is the initial stiffness, K_p is the plastic stiffness, M_0 is the reference moment, and N is the curve shape parameter. The model represents observed experimental results well and has been implemented in a computer program (Richard 1993). The physical definition of each parameter is shown in Fig. 1.

Eq. (11) represents the monotonically increasing loading section of the $M - \theta$ curves. In a typical dynamic analysis, at a given time, some of the PR connections are expected to be loading and others are expected to be unloading and reloading. Studies related to the unloading and reloading behavior at PR connections, both experimental and theoretical, are rare. The unloading and reloading behavior of the $M - \theta$ curves is essential. This subject was addressed recently in the literature (Colson 1991, El-Salti 1992). In these studies, the monotonic loading behavior and the Masing rule are used to theoretically develop the unloading and reloading sections of the $M - \theta$ curve. A general class of Masing models can be defined with a virgin loading curve as:

$$f(M, \theta) = 0 \tag{12}$$

and its unloading and reloading curve can be described by the following equation:

$$f\left(\frac{M - M_a}{2}, \frac{\theta - \theta_a}{2}\right) = 0 \tag{13}$$

where (M_a, θ_a) denotes the load reversal point as shown in Fig 2.

Using the Masing rule and the Richard Model represented by Eq. (11), the mathematical model used in this study for the unloading and reloading behavior of a PR connection is given by:

$$M = M_a - \left[\frac{(K - K_p)(\theta_a - \theta)}{\left(1 + \left|\frac{(K - K_p)(\theta_a - \theta)}{2M_0}\right|^N\right)^{\frac{1}{N}}}\right] - K_p (\theta_a - \theta) \tag{14}$$

If (M_b, θ_b) is the next reversal point, as shown in Fig. 2, the reloading relation between M and θ can be obtained by simply replacing (M_a, θ_a) with (M_b, θ_b) in Eq. (14). Thus, Eq. (11) is used if the connection is loading; if it is unloading or reloading, Eq. (14) should be used instead.

The hysteretic damping produced during the loading, unloading and reloading process of the

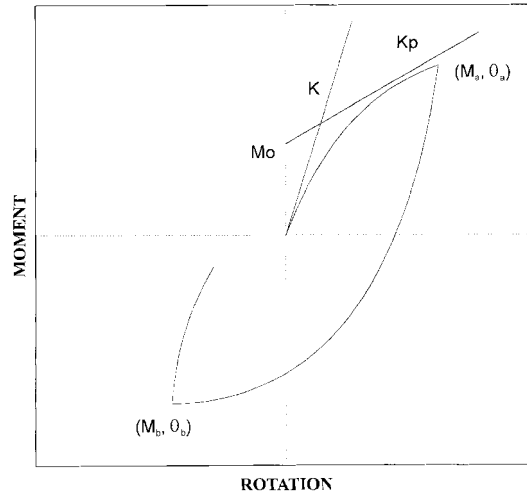


Fig. 2 Hysteretic behavior at PR connections

connections is illustrated in Fig. 2. This could be one of the most important sources of energy dissipation in the structure.

5. Mathematical formulation

To evaluate the different components of energy dissipation discussed earlier, an efficient finite element-based time-domain nonlinear analysis algorithm already developed by the authors is used (Gao and Haldar 1995, Reyes-Salazar and Haldar 1997). Considering its efficiency, particularly for steel frame structures, the assumed stress-based finite element method (Kondoh and Atluri 1987, Haldar and Nee 1989, Shi and Atluri 1988) is used. Using this approach, an explicit form of tangent stiffness can be derived. Fewer elements can be used in describing a large deformation configuration without sacrificing any accuracy, and the tangent stiffness matrix can be formulated without any integration. Furthermore, information on material nonlinearity and connection rigidity can be incorporated in the algorithm without losing its basic simplicity. It gives very accurate results and is very efficient compared to the displacement-based approach. The procedure has been carefully studied and verified. The algorithm will not be discussed further due to lack of space.

6. Structural model

To verify the mathematical model, a steel frame experimentally investigated by Leon and Shin (1995) is considered. It is a two-story two-bay frame, as shown in Fig. 3. The span of each bay is 4.06 m, and the story height is 1.88 m. W6×20 wide flange section is used for the exterior columns, and W6×25 is used for the interior columns. All beams are made of W8×18. All members are made of A36 steel. All connections consist of top and seat angles (L6×3 1/2×5/16) and web angles (2 – L3 1/2×2 1/2×1/4) and are made from A36 steel. The frame is assumed to be fixed at the base. Further details of the frame and connections can be obtained from Leon and Shin (1995).

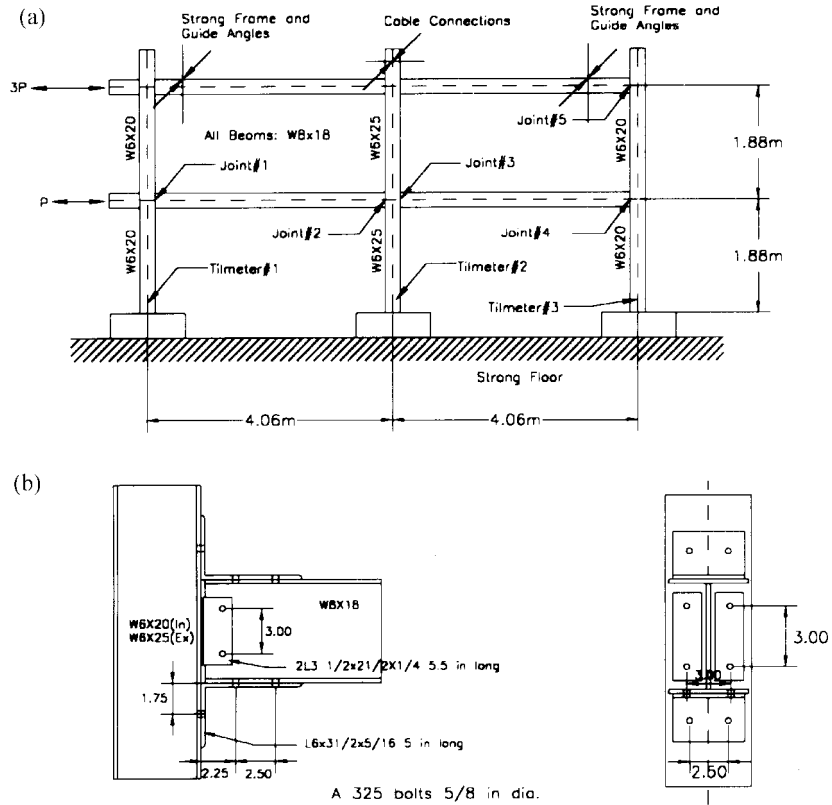


Fig. 3 (a) Frame, (b) Connection (Leon and Shin 1995)

All the connections are considered to be PR, and are represented by the Richard equation (Eq. 11). The experimental $M - \theta$ curve for the connections reported by Leon and Shin is shown in Fig. 4a. The Richard equation is used to analytically represent the monotonic behavior and is shown in Fig. 4b. Both curves match very well.

To define the connection rigidity, a parameter called the T ratio is introduced. It is the ratio of the

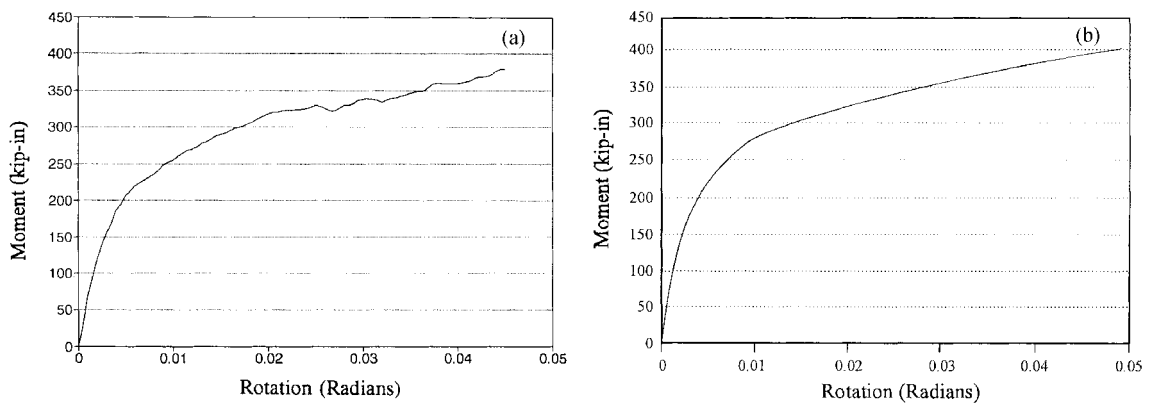


Fig. 4 (a) Experimental $M - \theta$ curve, (b) Analytical $M - \theta$ curve

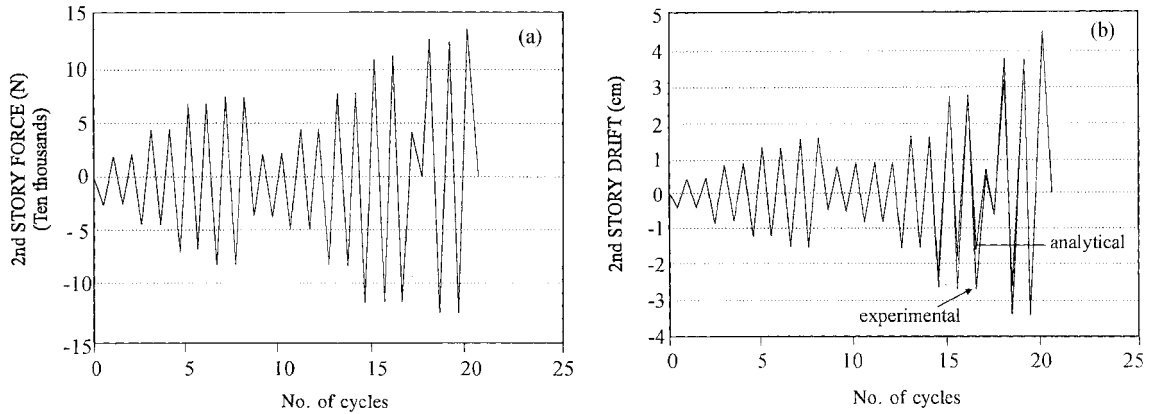


Fig. 5 (a) Lateral load, (b) Experimental and analytical second story drift

moment the connection would have to carry according to the beam line theory (Disque 1964) and the fixed end moment of the girder. A T ratio greater than 0.9 generally represents a fully restrained connection. Using the Richard curve, the T ratio for the connections is found to be 0.3, representing a very flexible connection.

7. Verification of the analytical model

A very elaborate nonlinear finite element computer program developed by the authors and their colleagues (Gao and Haldar 1995, Reyes-Salazar and Haldar 1997) is used for verification purposes. This program was verified for dynamic and seismic loadings, and the results were extensively reported in the literature.

Leon and Shin (1995) applied laterally proportional story load with a ratio of 3:1, and reported the experimental results of the second story force and the corresponding drift shown in Figs. 5a and 5b, respectively. The test frame was subjected to a total of 20 cycles of loading. The intensity of the load was changed from cycle to cycle as shown in Fig. 5a. The analytical results obtained using the algorithm are shown in Fig. 5b. The experimental and analytical results for 18 load cycles are almost identical. The analytical model appears to be reasonable.

The verified model is then used to quantify energy dissipation for different parameters identified in Eq. (1).

8. Results and observations

The frame discussed above is considered again. The frame is first excited laterally at the top by a sinusoidal load of the form $p(t) = P_0 \sin \omega t$, where P_0 is the amplitude of the load and ω is the frequency of excitation. This will be denoted as Load Case 1 in the subsequent discussion. The frame is then subjected laterally to a base sinusoidal ground acceleration of the form $\ddot{u}(t) = \ddot{u}_0 \sin \omega t$, representing a seismic excitation, where \ddot{u}_0 is the amplitude of the sinusoidal acceleration. This will be denoted hereafter as Load Case 2. The frequencies are the same for both load cases. Both load

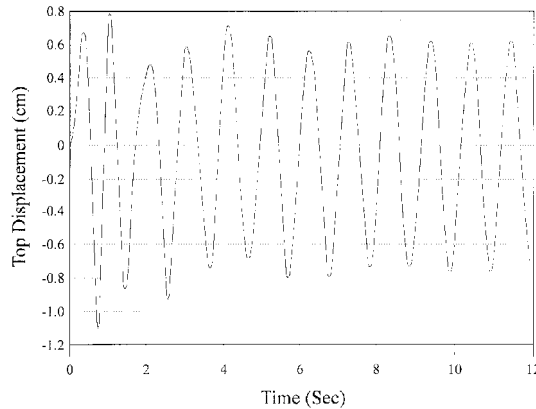


Fig. 6 Response of the frame in terms of the top displacement

cases produced similar lateral displacements for the frame.

The top lateral displacement of the frame for a load P_0 of 22,500 N, a frequency ω of 6 rad/sec, ζ (viscous damping expressed in terms of percent of the critical damping) of 2%, and a T ratio of 0.3 is shown in Fig. 6. The lateral displacement approaches the steady state after the transient response. The energy dissipation for each source, to be presented in subsequent discussion, is calculated per cycle in the steady state phase of the response.

Eq. (10) can be used to estimate energy dissipation at the PR connections considering moment, shear and axial forces. However, after extensive study, it is observed that the energy dissipation due to shear and axial forces is negligible compared to that due to moment. This is because the shear and axial load deformation behaviors are linear, and the corresponding energy dissipation due to hysteretic behavior can be neglected. Therefore, only the energy dissipation due to moment at the PR connections is reported in this paper.

To make the observations meaningful P_0 , \ddot{u} , ω , ζ , and the T ratio are selected for the parametric study. For each combination of these parameters, all the terms in Eq. (1) are calculated. The maximum top lateral displacement of the frame, d_{\max} , E_D , E_C , and E_P (if plastic hinges are formed) are presented in this paper.

The results for P_0 of 8100 N, ω of 3, 6, and 9 rad/sec, ζ of 1, 2, 5, and 10%, and a T ratio of 0.3 are presented in Table 1 for both load cases. The fundamental frequency of the frame, ω_n , with a connection stiffness represented by the T ratio of 0.3, is found to be 10.6 rad/sec. The flexible frame did not develop any plastic hinges, and thus E_P is not shown in Table 1. If the magnitude of the sinusoidal load is increased, the frame fails by developing very large lateral displacements without forming plastic hinges.

To study the significance of energy dissipation at the PR connections relative to that due to viscous damping, a parameter R_1 is introduced. It is calculated as $R_1 = E_C/E_D \times 100$, and is shown in Table 1. Several important observations can be made from the results given in Table 1. As expected, for a given ω , d_{\max} and E_C decrease and E_D increases with an increase in the damping values. Also, as ω decreases, indicating movement away from the resonance condition, the d_{\max} values decrease. The R_1 values are large, particularly for the low damping values expected in a typical steel frame, indicating that the dissipation of energy at PR connections may be comparable to that dissipated by viscous damping. Also, if d_{\max} and the rotation at the PR connections remain large, either due to low damping or as it approaches the resonance condition, the energy dissipation at the PR con-

Table 1 Energy dissipation at PR connections for $T = 0.3$, $P_0 = 8100$ N and $\ddot{u}_0 = 38$ cm/Sec²

ω (rad/Sec) (1)	ξ (%) (2)	Load applied at the top story				Load applied at the base			
		d_{\max} (cm) (3)	E_C (N-m) (4)	E_D (N-m) (5)	R_1 (%) (6)	d_{\max} (cm) (7)	E_C (N-m) (8)	E_D (N-m) (9)	R_1 (%) (10)
9	1	3.06	22.37	25.43	87.97	2.45	24.41	26.67	91.53
	2	2.30	21.70	51.98	41.75	2.28	23.73	46.90	50.60
	5	1.88	15.59	112.55	13.85	1.86	20.34	104.53	19.46
	10	1.45	6.78	170.18	3.98	1.43	14.92	158.87	9.39
6	1	0.96	1.02	6.78	15.04	0.95	1.22	3.94	30.96
	2	0.94	0.81	14.67	5.52	0.92	1.15	5.82	19.76
	5	0.88	0.41	37.90	1.08	0.86	1.02	13.52	7.54
	10	0.79	0.20	73.36	0.27	0.78	0.95	25.12	3.78
3	1	0.66	0.34	5.32	6.39	0.53	0.29	3.63	7.99
	2	0.61	0.27	10.14	2.66	0.48	0.28	5.34	5.24
	5	0.53	0.14	25.40	0.55	0.43	0.26	8.63	3.01
	10	0.46	0.07	48.55	0.14	0.38	0.24	15.09	1.59

nections becomes significant. Thus, large deformation of the frame is essential to have significant energy dissipation at the PR connections. The results are similar for both load cases.

To study the effect of the stiffness of PR connections in dissipating energy, the same frame is considered again with stiffer connections given by the T ratio of 0.6 and 0.9. The fundamental frequencies of the frame with these connections are 12.8 and 13.9 rad/sec, respectively. The frame is excited by the same loads as shown in Table 2. The frame did not develop any plastic hinges for both load cases. Results for the T ratio of 0.6 are shown in Table 2. It can be observed that E_C and R_1 decrease significantly as the stiffness of the connections increases. Again, the results are very similar for both load cases. The results for the frame with a T ratio of 0.9 are not shown here due to lack of space. However, both E_C and R_1 are practically zero for this case.

To observe the influence of connection stiffness on the energy dissipation at the PR connections, the

Table 2 Energy dissipation at PR connections for $T = 0.6$, $P_0 = 8100$ N and $\ddot{u}_0 = 38$ cm/Sec²

ω (rad/Sec) (1)	ξ (%) (2)	Load applied at the top story				Load applied at the base			
		d_{\max} (cm) (3)	E_C (N-m) (4)	E_D (N-m) (5)	R_1 (%) (6)	d_{\max} (cm) (7)	E_C (N-m) (8)	E_D (N-m) (9)	R_1 (%) (10)
9	1	0.86	0.420	24.88	1.69	0.82	.87	33.32	2.61
	2	0.85	0.322	81.33	0.40	0.76	.81	88.63	0.91
	5	0.84	0.345	202.06	0.17	0.72	.73	275.50	0.26
	10	0.83	0.299	383.80	0.08	0.69	.71	409.78	0.17
6	1	0.49	0.067	11.45	0.59	0.51	.12	15.34	0.78
	2	0.46	0.059	24.11	0.24	0.49	.11	31.23	0.35
	5	0.45	0.059	58.63	0.10	0.44	.09	59.32	0.15
	10	0.44	0.054	116.11	0.05	0.42	.08	124.21	0.06
3	1	0.41	0.018	4.12	0.44	0.43	.04	7.62	0.52
	2	0.40	0.018	8.03	0.22	0.39	.04	16.10	0.25
	5	0.39	0.017	20.68	0.08	0.34	.03	32.89	0.09
	10	0.39	0.017	41.38	0.04	0.29	.02	68.23	0.03

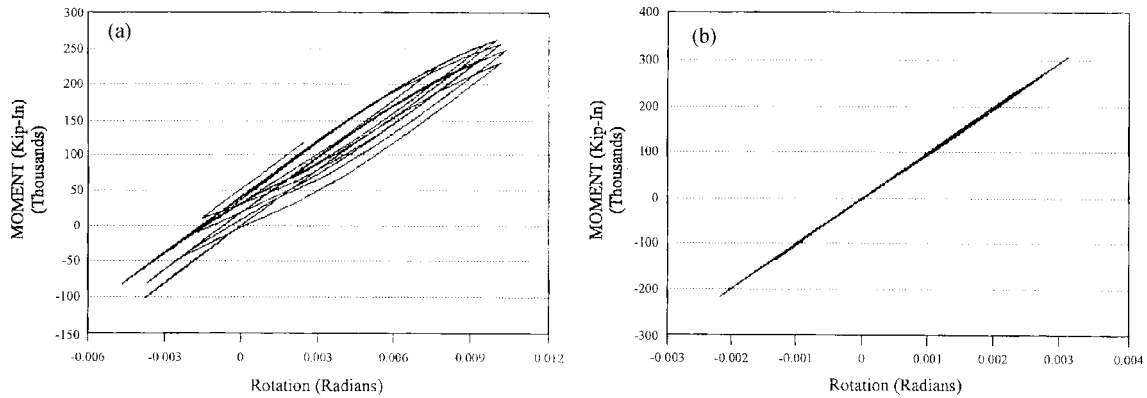


Fig. 7 Moment rotation hysteretic behavior, (a) $T = 0.3$, (b) $T = 0.6$

moment and the corresponding rotation at the PR connection obtained at the top left hand joint of the second floor for Load Case 1 with P_0 of 8100 N, ω of 9 rad/sec, ζ of 2% damping and the T ratio of 0.3 and 0.6 are plotted in Fig. 7 for a few cycles of vibration. It is clear that the dissipated energy (area under the $M - \theta$ curve) is much larger for the case where the connections are more flexible.

To study the effect of deformation of the frame (lateral displacement and rotation at the PR connections), the same frame is considered with three different connection stiffnesses. In Load Case 1, three different load amplitudes (P_0) of 8100, 22500, and 33375 N are used to excite the frame. In Load Case 2, three acceleration levels of 38, 104, and 155 cm/sec^2 are used. Results for the T ratio of 0.3 are given in Table 3. As in the previous cases, the frame did not develop any plastic hinges and consequently E_P was not calculated. Again, the results demonstrate that if the frame undergoes significant deformation, the energy dissipated at PR connections is comparable to that dissipated by viscous damping. For low values of damping and away from the resonance condition, E_C may even be larger than E_D , as shown in Table 3 for ω of 6 and 3 rad/sec and for 1 and 2% damping. It is

Table 3 Energy dissipation at PR connections for $T = 0.3$, P_0 and \ddot{u}_0 variable

ω (rad/Sec) (1)	ξ (%) (2)	Load applied at the story top					Load applied at the base				
		P_0 (N) (3)	d_{\max} (cm) (4)	E_C (N-m) (5)	E_D (N-m) (6)	R_1 (%) (7)	u_0 (cm/Sec ²) (8)	d_{\max} (cm) (9)	E_C (N-m) (10)	E_D (N-m) (11)	R_1 (%) (12)
9	1	8100	3.06	22.37	25.43	87.97	38	2.45	24.41	26.67	91.53
	2	8100	2.30	21.70	51.98	41.75	38	2.28	23.73	46.90	50.60
	5	8100	1.88	15.59	112.55	13.85	38	1.86	20.34	104.53	19.46
	10	8100	1.45	6.78	170.18	3.98	38	1.43	14.92	158.87	9.39
6	1	22500	2.83	42.04	13.33	315.27	104	2.73	31.87	30.73	103.71
	2	22500	2.76	40.68	44.07	92.31	104	2.65	30.51	43.05	70.87
	5	22500	2.56	35.93	107.01	33.58	104	2.46	29.83	98.20	30.38
	10	22500	2.30	31.19	205.77	15.16	104	2.21	29.83	187.70	15.89
3	1	33375	2.51	77.29	11.41	677.39	155	2.36	48.82	12.65	385.93
	2	33375	2.35	73.90	28.14	262.62	155	2.18	47.46	33.84	140.25
	5	33375	2.25	72.55	68.48	105.94	155	2.10	46.10	76.22	60.48
	10	33375	2.21	69.83	134.58	51.89	155	2.06	43.39	148.03	29.31

observed from Table 3 that E_C tends to increase and E_D tends to decrease as ω decreases. The corresponding R_1 value also increases as ω decreases. This is expected. As the frame moves away from the resonance condition, the effect of damping becomes less important. For low damping values, E_C becomes more significant than E_D .

The frame with stiffer PR connections, i.e., the T ratio of 0.6 and 0.9 is also studied. The observations made in Table 3 are still valid. The only additional observation is that the R_1 values still significant but are smaller than those for the T ratio of 0.3. This result is also expected and is noted in comparing Tables 1 and 2.

In all the cases discussed earlier, plastic hinges did not form in the frame. To study the effect of energy dissipation at the plastic hinges, and its significance with respect to energy dissipation at the PR connections and due to damping, the same frame with a T ratio of 0.9 is considered. The magnitudes of the sinusoidal load and the acceleration are adjusted so that the frame develops two or three plastic hinges, and the energy dissipated in them, E_P , is calculated. E_P values will increase as the frame develops more plastic hinges on its way to failure. The E_P values presented here indicate that they are close to the lower limit.

For ease of discussion, two additional parameters, R_2 and R_3 , are introduced. R_2 represents the ratio of the energy dissipated at PR connections, E_C , to that at plastic hinges, E_P or $R_2 = E_C/E_P \times 100$, indicating their relative importance. R_3 represents the ratio of the energy dissipated at plastic hinges, E_P , to that by viscous damping, E_D or $R_3 = E_P/E_D \times 100$, again indicating their relative importance.

The results are summarized in Table 4. Table 4 validates all the observations made on R_1 in the previous cases. As expected, E_P values decrease as damping increases. It is observed that E_C is comparable to E_P . It is important to note that the E_P values shown are close to the lower limit. E_C becomes less significant relative to E_P if more plastic hinges develop as the frame approaches failure. The R_2 and R_3 values shown in Table 4 are close to the upper and lower bounds, respectively. For low damping values, the dissipation of energy at plastic hinges is comparable to, and sometimes larger than that due to viscous damping. However, as the magnitudes of the sinusoidal loads increase for both load cases, the energy dissipation at plastic hinges also increases. This is

Table 4 Energy dissipation at PR connections for $T = 0.9$, P_0 and \ddot{u}_0 variable

ω (rad/ Sec) (1)	ξ (%) (2)	Load applied at top story									Load applied at the base						
		P_0 (N) (3)	d_{max} (cm) (4)	E_C (N-m) (5)	E_D (N-m) (6)	E_P (N-m) (7)	R_1 (%) (8)	R_2 (%) (9)	R_3 (%) (10)	\ddot{u}_0 (cm/ Sec ²) (11)	d_{max} (cm) (12)	E_C (N-m) (13)	E_D (N-m) (14)	E_P (N-m) (15)	R_1 (%) (16)	R_2 (%) (17)	R_3 (%) (18)
9	1	36156	4.65	81.70	197.61	84.47	41.34	96.72	42.75	156	3.83	128.37	969.65	546.81	13.24	23.48	56.39
	2	36156	4.55	80.34	398.18	66.25	20.18	121.27	16.64	156	3.78	136.50	1,241.08	305.10	11.00	44.74	24.58
	5	36156	4.29	70.43	1,056.21	42.86	6.67	164.33	4.06	156	3.56	115.71	1,791.39	83.85	6.46	138.00	4.68
	10	36156	3.58	54.75	2,056.34	16.60	2.66	329.82	0.81	156	3.30	92.21	2,522.27	0.00	3.66	*	0.00
6	1	54234	4.90	97.90	101.90	259.97	96.07	37.66	255.12	235	3.61	93.84	1,215.85	292.24	7.72	32.11	24.04
	2	54234	4.62	98.72	286.04	168.80	34.51	58.48	59.01	235	3.53	94.92	1,332.43	244.03	7.12	38.90	18.31
	5	54243	4.39	94.78	787.66	86.54	12.03	109.52	10.99	235	3.43	96.73	1,733.64	128.19	5.58	75.46	7.39
	10	54234	3.76	87.33	1,582.58	61.72	5.52	141.49	3.90	235	3.30	97.09	2,263.12	117.07	4.29	82.93	5.17
3	1	76206	4.65	109.84	81.20	392.17	135.27	28.01	482.97	255	3.51	88.14	299.74	352.67	29.41	24.99	117.66
	2	76206	4.50	110.18	170.18	227.13	64.74	48.51	133.46	255	3.48	75.03	468.79	406.91	16.01	18.44	86.80
	5	76206	4.39	110.52	422.28	112.38	26.17	98.34	26.61	255	3.43	77.29	799.14	124.41	9.67	62.13	15.57
	10	76206	3.96	106.45	1,852.12	74.30	5.75	143.27	4.01	255	3.23	62.38	1,131.35	0.00	5.51	*	0.00

* = no plastic hinge was developed.

Table 5 Energy dissipation of the frame with FR connections

ω (rad/Sec) (1)	ξ (%) (2)	Load applied at top story					Load applied at the base					
		P_0 (N) (3)	d_{\max} (cm) (4)	E_D (N-m) (5)	E_P (N-m) (6)	R_3 (N-m) (7)	\ddot{u}_0 (cm/Sec ²) (8)	d_{\max} (cm) (9)	E_D (N-m) (10)	E_P (N-m) (11)	R_3 (%) (12)	
9	1	36156	4.22	98.00	69.71	71.13	156	3.43	343.86	198.77	57.81	
	2	36156	4.06	324.16	13.87	4.28	156	3.35	1,040.62	69.61	6.69	
	5	36156	3.86	822.11	6.16	0.75	156	3.20	1,212.83	20.00	1.65	
	10	36156	3.56	1,590.26	*		156	2.97	1,365.83	*		
6	1	54234	4.52	34.91	122.64	351.30	235	3.53	341.96	262.82	76.86	
	2	54234	4.08	241.43	50.28	20.83	235	3.33	746.93	112.75	15.10	
	5	54234	4.01	655.55	28.52	4.35	235	3.25	987.60	49.49	5.01	
	10	54234	3.93	1,336.44	18.17	1.36	235	3.18	1,298.91	28.95	2.23	
3	1	76206	4.19	37.91	189.41	499.63	255	3.45	91.70	429.12	467.96	
	2	76206	4.06	95.53	67.66	70.83	255	3.33	210.52	163.40	77.62	
	5	76206	3.96	328.49	23.83	7.25	255	3.12	458.16	14.86	3.24	
	10	76206	3.90	695.12	7.98	1.15	255	2.92	620.26	*		

* = no plastic hinge was developed

expected since the number of plastic hinges in the frame also increases.

From a practical point of view, the profession considers a PR connection with a T ratio of at least 0.9 to be a fully restrained (FR) connection. However, it is recognized that there is some flexibility in such a rigid connection. In order to study the simplified assumption routinely made in analyzing such a frame, the frame used to generate Table 4 is considered again, except that all the connections are assumed to be conventional FR type; in other words, the T ratio is 1.0 (i.e., the relative rotation between the beams and columns is zero). The fundamental frequency of the frame is found to be 14.27 rad/sec.

The results for this case are shown in Table 5. R_1 and R_2 can not be calculated for this frame, since E_C does not exist. Therefore, only the E_D and E_P values and the corresponding R_3 values are calculated and shown in Table 5. Again, R_3 represents a value close to the lower bound. As expected, d_{\max} values went down for the frame with FR connections, effectively reducing the input energy. However, this reduced energy needs to be dissipated using sources of dissipation other than E_C . As the magnitude of the sinusoidal load increases, the number of plastic hinges in the frame increase, and E_P values go up, approaching the upper limit. When the damping is more than 2%, E_P is not significant compared to E_D . On the other hand, when the same frame is modeled as consisting of PR connections with a T ratio of 0.9, the input energy is larger than for the frame with PR connections. A significant portion of this increase is dissipated by the PR connections.

The results shown in Tables 4 and 5 indicate that for the frame with T ratio of 0.9 and 1.0, the major source of energy dissipation is damping, particularly for high damping values. By comparing Tables 4 and 5, it is also observed that the values of d_{\max} , E_D , and E_P are smaller for the frame with FR connections than for the frame with PR connections. These observations are expected.

9. Conclusions

The major sources of energy dissipation in steel frames with partially restrained (PR) connections are studied. Available experimental results are used to verify the mathematical model used in this

study. The verified model is then used to quantify the energy dissipation in PR connections due to viscous damping and at plastic hinges if they form. Observations are made for two load conditions: a sinusoidal dynamic load applied at the top of the frame, and a sinusoidal ground acceleration applied at the base of the frame representing the seismic loading condition. This analytical study confirms, in general, the behavior observed during experimental investigations: that PR connections reduce the overall stiffness of frames, but add a major source of energy dissipation. This is particularly significant if the connections are very flexible. However, a frame with flexible connections must satisfy the lateral deformation requirements. As the connections become stiffer, the contribution of PR connections to energy dissipation becomes less significant. It is found that the energy dissipation behavior is different for a frame with FR connections, i.e., with a T ratio of 1.0, and the same frame with PR connections, i.e., with a T ratio of 0.9. Considering the practical design aspect, a connection with a T ratio of at least 0.9 cannot be considered to be a FR connection, particularly for dynamic and seismic response analysis. It is also observed that a frame containing PR connections with different rigidities will alter its fundamental frequency. Depending on the situation, it may bring the frame closer to or further from the resonance condition. If the frame approaches the resonance condition, the effect of damping is expected to be very important. However, if the frame moves away from the resonance condition, the energy dissipation at the PR connections is expected to be significant for an increase of the frame deformation, particularly for low damping values. For low damping values, the dissipation of energy at plastic hinges is comparable to that due to the viscous damping and increases as the frame approaches failure. For the range of parameters considered in this study, the energy dissipations at the PR connections and at the plastic hinges are of the same order of magnitude. The study quantitatively confirms the general observations made in experimental investigations for frames with PR connections; however, proper consideration of the stiffness of PR connections and other dynamic properties are essential for predicting dynamic behavior.

Acknowledgements

This paper is based on work partly supported by the National Science Foundation under Grant No. CMS-9526809. The work is also partially supported by El Consejo Nacional de Ciencia y Tecnología (CONACYT), México and La Universidad Autónoma de Sinaloa (UAS), México. The authors would like to thank Prof. Roberto T. Leon of Georgia Institute of Technology for providing essential information on tests that he and his research associates conducted in their laboratory. Any opinions, findings, conclusions or recommendations expressed in this publication are those of the authors and do not necessarily reflect the views of the sponsors.

References

- Chen, W.F. and Lui, E.M. (1987), "Effects of joint flexibility on the behavior of steel frames", *Computers and Structures*, **26**(5), 719-732.
- Colson, A. (1991), "Theoretical modeling of semirigid connections behavior" *Journal of the Construction Steel Research*, **19**, 213-224.
- Disque, R.O. (1964), "Wind connections with simple framing", *Engineering Journal*, AISC, **1**(3), 101-103.
- El-Salti, M.K. (1992), "Design of frames with partially restrained connections", PhD Thesis, Department of Civil Engineering and Engineering Mechanics, University of Arizona.

- Fry, M.J. and Morris, G.A. (1975), "Analysis of flexibly connected steel frames", *Canadian Journal of Civil Engineering*, **2**(3), 280-291.
- Gao, L. and Haldar, A. (1995), "Safety evaluation of frames with PR connections", *Journal of Structural Engineering*, ASCE, **121**(7), 1101-1109.
- Haldar, A. and Nee, K.-M. (1989), "Elasto-plastic large deformation analysis of PR steel frames for LRFD", *Computers & Structures*, **31**(5), 811-823.
- Haldar, A. and Reyes, S.A. (1996), "Ductility evaluation of steel frames with PR connections", *Eleventh World Conference on Earthquake Engineering*, Paper No. 1903.
- Kawamura, H. and Galambos, T.V. (1989), "Earthquake load for structural reliability", *Journal of Structural Engineering*, ASCE, **115**(6), 1446-1462.
- Kondoh, K. and Atluri, S.N. (1987), "Large deformation, elasto-plastic analysis of frames under non-conservative loading, using explicitly derived tangent stiffness based on assumed stress", *Computational Mechanics Journal*, **2**(1), 1-25.
- Leger, P. and Dussault, S. (1992), "Seismic-energy dissipation in MDOF structures", *Journal of Structural Division*, ASCE, **118**(5), 1251-1269.
- Leon, R.T. and Shin, K.J. (1995), "Performance of semi-rigid frames", *Proceedings of Structure Congress*, 1020-1035, April.
- Nader, M.N. and Astaneh, A. (1991), "Dynamic behavior of flexible, semirigid and rigid frames", *Journal of Construction Steel Research*, **18**, 179-192.
- Reyes-Salazar, A. and Haldar, A. (1997), "Inelastic nonlinear seismic response and ductility evaluation of steel frames with fully, partially restrained and composite connections", *Report No. CEEM-97-01*, Department of Civil Engineering and Engineering Mechanics, University of Arizona, Tucson, AZ.
- Reyes-Salazar, A. and Haldar, A. (1999), "Nonlinear seismic response of steel structures with PR and composite connections", *Journal of Constructional Steel Research*, **51**(1), 37-59.
- Richard, R.M. (1986), "Single-plate framing connection designs", *The National Engineering Conference*, June.
- Richard, R.M., PRCONN (1993), "Moment-rotation curves for partially restrained connections", *RMR Design Group*, Tucson, Arizona.
- Shi, G. and Atluri, S.N. (1988), "Elasto-plastic large deformation analysis of space-frames", *International Journal for Numerical Methods in Engineering*, **26**, 589-615.
- Uang, C.M. and Bertero, V.V. (1990), "Evaluation of seismic energy in structures", *Journal of Earthquake Engineering and Structural Dynamics*, **19**, 77-90.

Notations

- d_{\max} = maximum top lateral displacement
 E_C = energy dissipated at PR connections
 E_D = energy dissipated by viscous damping
 E_P = energy dissipated at plastic hinges
 E_I = input energy
 ξ = percent of the critical damping
 E_K = kinetic energy
 E_S = elastic strain energy
 E_P = plastic energy
 E_D = energy dissipated by viscous damping
 E_C = energy dissipated at PR connections
 H_P = plastic axial elongation
 K = initial stiffness of connections
 K_P = plastic stiffness

- M = moment of the connection
- M_0 = reference moment
- M_P = bending moment when yield occurs
- N = shape parameter for connections
- P_0 = amplitude of the sinusoidal excitation
- P_P = axial load when yield occurs
- R_1 = ratio of E_C to E_D
- R_2 = ratio of E_C to E_P
- R_3 = ratio of E_P to E_D
- θ = relative rotation of connections
- θ_p = plastic rotation
- ω = frequency of the sinusoidal excitation
- ω_n = fundamental frequency of the frames
- T = relative stiffness of connections